

Articles

Recombinant Protein-co-PEG Networks as Cell-Adhesive and Proteolytically Degradable Hydrogel Matrixes. Part I: Development and Physicochemical Characteristics

Simone C. Rizzi[†] and Jeffrey A. Hubbell^{*,†,‡}

Department of Materials and Integrative Biosciences Institute, Ecole Polytechnique Fédérale de Lausanne (EPFL) and University of Zurich, Switzerland, and Institute for Biological Engineering and Biotechnology, Swiss Federal Institute of Technology Lausanne (EPFL), CH-1015 Lausanne, Switzerland

Received July 4, 2004; Revised Manuscript Received January 10, 2005

Toward the development of synthetic bioactive materials to support tissue repair, we present here the design, production, and characterization of genetically engineered protein polymers carrying specific key features of the natural extracellular matrix, as well as cross-linking with functionalized poly(ethylene glycol) (PEG) to form hybrid hydrogel networks. The repeating units of target recombinant protein polymers contain a cell-binding site for ligation of cell-surface integrin receptors and substrates for plasmin and matrix metalloproteinases (MMPs), proteases implicated in wound healing and tissue regeneration. Hydrogels were formed under physiological conditions via Michael-type conjugate addition of vinyl sulfone groups of end-functionalized PEG with thiols of cysteine residues, representing designed chemical cross-linking sites within recombinant proteins. Cross-linking kinetics was shown to increase with the pH of precursor solutions. The elastic moduli (G') and swelling ratios (Q_m) of the resulting hydrogels could be varied as a function of the stoichiometry of the reacting groups and precursor concentration. Optima of G' and Q_m , maximum and minimum, respectively, were obtained at stoichiometry ratios r slightly in excess of 1 (r = cysteine/vinyl sulfone). The pool of technologies utilized here represents a promising approach for the development of artificial matrixes tailored for specific medical applications.

Introduction

New challenges in therapeutic tissue regeneration call for development of synthetic material systems that control the natural environment and can be adapted to specific biological contexts.^{1–5} Major efforts are being directed toward designing synthetic matrixes that mimic the extracellular matrix to actively interact with living tissues.^{6–10} To achieve dynamic interactions with cells and induce specific cell and tissue responses, biomaterials are being developed to incorporate defined biomolecular species, such as adhesion ligands and growth factors, for signaling through biological recognition. Furthermore, materials are being designed to remodel proteolytically^{6–10} (i.e., in response to enzymes secreted locally by adjacent cells^{11–13} rather than by chemical hydrolysis) to harness natural signals of tissue regeneration and wound healing processes. Presently, natural matrixes, such as fibrin and collagen, represent the gold standard for therapeutic tissue regeneration.^{14–16} However, these natural matrixes have several potential disadvantages, such as a risk

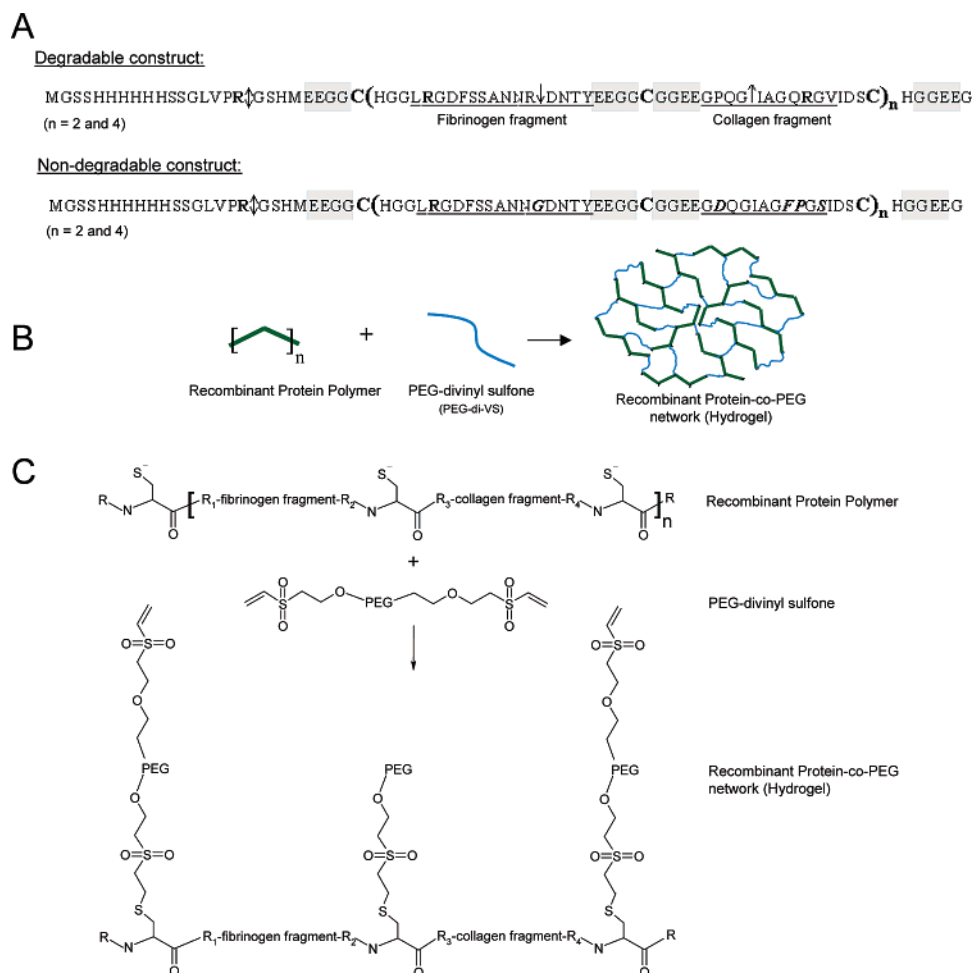
of infectious agent transfer and difficulty in adaptation to a specific biological application.^{17,18}

The approach pursued here was inspired by the two-component hybrid hydrogel family consisting of recombinant proteins and synthetic hydrophilic polymers pioneered by Kopecek and co-workers,¹⁹ as well as by recombinant DNA methodology for the production of protein polymers developed by Tirrell et al.^{20–23} and by Ferrari and Cappello and their collaborators.^{24–26} Our intent was to start from a bioinert polymer such as poly(ethylene glycol) (PEG) and add desired biological functionality by cross-linking PEG with engineered protein polymers. Thus, in our approach, the protein polymer provides two functions: it serves as a cross-linker to react with functionalized PEG to yield an elastic gel after mixing two inviscid liquids, and it supplies biological functionality. Templates for the protein component are small functional oligopeptide building blocks derived from natural proteins.²⁷ As previously reported, recombinant DNA technology enables the de novo design and bacterial synthesis of protein polymers consisting of specific combinations of functional oligopeptide blocks.^{28–32} The functionalized protein polymers produced in this study contain two key elements that are characteristic for natural extracellular matrixes and necessary to support cell migration within three-dimensional (3-D)

* Corresponding author. Telephone: +41 21 693 9681; fax: +41 21 693 9665; e-mail: jeffrey.hubbell@epfl.ch.

[†] Swiss Federal Institute of Technology Zurich (ETHZ) and University of Zurich.

[‡] Ecole Polytechnique Fédérale de Lausanne.

Chart 1. (A) Degradable and Nondegradable Recombinant Protein Polymer Constructs,^a (B) Hydrogel Formation Schema, and (C) Details of Chemical Reaction

^a One letter amino acid code: alanine (A), arginine (R), asparagine (N), aspartic acid (D), cysteine (C), glutamic acid (E), glutamine (Q), glycine (G), histidine (H), isoleucine (I), leucine (L), lysine (K), methionine (M), phenylalanine (F), proline (P), serine (S), threonine (T), tryptophan (W), tyrosine (Y), and valine (V). (double-headed vertical arrow) Thrombin-cleavable site for N-terminal hexahistidine tag removal. (↓) Designed plasmin degradation site. (R) Additional potential plasmin degradation positions (at arginine C-terminus; see Experimental Procedures). (†) Designed matrix metalloproteinase (MMP) cleavage sequence.

matrixes:³³ (i) a cell adhesion motif and (ii) protease-cleavable sites. As to the cross-linking function of the protein polymer, interspersed chemically reactive sites in the protein backbone enable the formation of elastic hydrogels through chemical reaction with the reactive end-groups of functionalized PEG.

Specifically, the monomer of the expressed protein constructs (Chart 1A) consists of 15 amino acids based on human fibrinogen (α -chain, residue L⁹⁴-Y¹⁰⁸ underlined),³⁴ including the cell adhesion sequence RGD and a plasmin degradation site (cleavage site indicated by ↓). Also included are 11 amino acids (underlined) corresponding to a matrix metalloproteinase (MMP) cleavage sequence (indicated by †) existing in human collagen (α 1(I) chain, residue G⁹⁵⁰-V⁹⁶⁰).³⁵ Blocks of charged amino acids (glutamic acid, E) within the protein backbone (shaded) were added to enhance protein solubility. A thrombin-cleavable (double-headed vertical arrow) hexahistidine tag placed at the N-terminus of the recombinant target proteins facilitates their purification from the bacterial lysate via nickel-affinity chromatography. Thiol groups of cysteine residues serve as chemically reactive cross-linking sites and are located between the degradation sites and at both termini of the repeating unit (cysteine, C). In particular,

under physiological conditions, thiolates from cystyl residues react with vinyl sulfone groups of correspondingly functionalized PEG (PEG-di-VS). The high selectivity and mild nature of the reaction between the cystyl thiol and the vinyl sulfone on the PEG^{36,37} enables the formation of a bioactive synthetic network by liquid-to-solid transformation in situ (i.e., in the presence of living cells and tissues (Chart 1B,C)). A second construct, differing only in the sensitivity to degradation, is also shown in Chart 1A (nondegradable protein construct). Both the plasmin and the MMP cleavage sites were mutated and rendered nondegradable (substituted amino acids are in italics and are bolded).

The materials investigated here belong to a family of PEG-based hybrid matrixes introduced by West and Hubbell⁶ designed to mimic some key features of ECMs including susceptibility to proteolytic degradation. Different approaches have been utilized for their production. In particular, the production methods of the materials of this paper differ from those of West and Hubbell⁶ in the cross-linking chemistry as well as the methods of precursor preparation. Photopolymerization of acrylate groups has been used by West and Hubbell⁶ and Gobin and West⁸ as well as by Halstenberg et al.⁷ to produce polymer networks consisting of PEG-

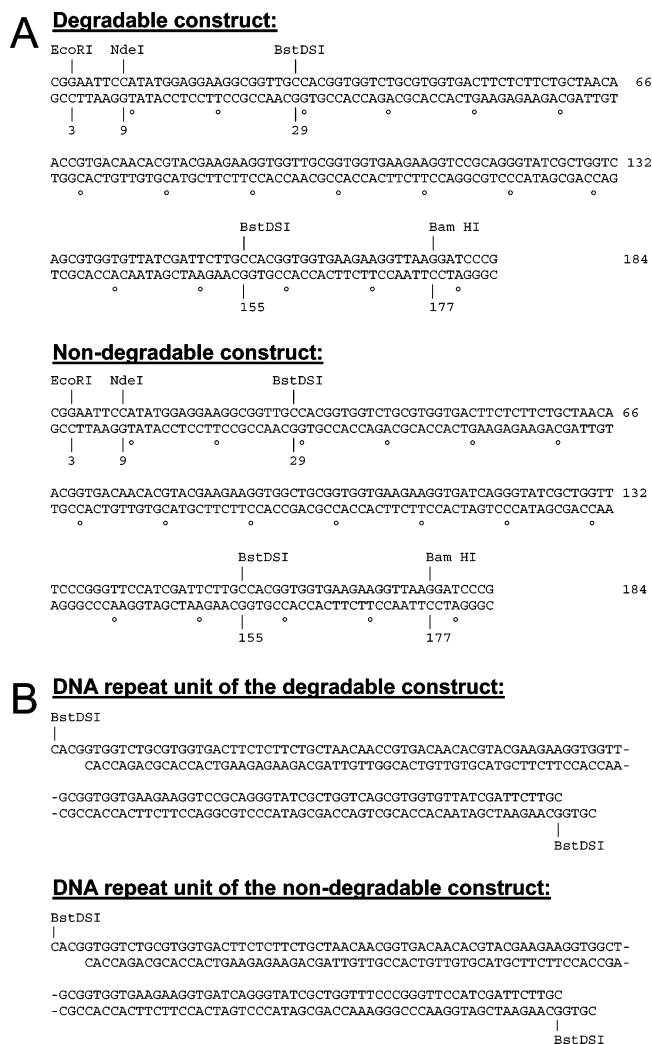
grafted synthetic oligopeptides^{6,8} and PEG-grafted recombinant protein polymers,⁷ respectively. Lutolf et al. utilized the Michael-type conjugate addition of cysteine thiols to vinyl sulfone functional groups to cross-link multi-armed PEG macromers and cysteine-containing oligopeptides by stepwise copolymerization.^{9,10} We present herein a combination of the approaches followed by Halstenberg et al.⁷ and Lutolf and Hubbell,⁹ thus taking advantages of genetic engineering versus chemical synthesis for the production of much more complicated and sophisticated biomolecular components, and of Michael-type conjugate addition reactions as a means toward cross-linking, for formation of the actual material from two liquid precursors. In this paper, we describe the design, production, and characterization of proteolytically sensitive and cell adhesive artificial protein polymers for use as cross-linkable hydrogel precursors. Furthermore, we present reaction and material properties, including the influence of pH on the rate of cross-linking as well as the dependence of final physicochemical properties on preparation conditions.

Experimental Procedures

Standard techniques were used for DNA design and manipulation, bacterial protein expression, and protein characterization. Polymerase chain reactions (PCR) were performed with PCR Sprint (Hybaid), using the polymerase Deep Vent (New England Biolabs) at 80 mU/ μ L in the recommended buffer and 6 mM MgSO₄. Amplification by PCR occurred over 30 cycles for 30 s at 94 °C for denaturation, 15 s between 50 and 56 °C for annealing, and 15 s at 72 °C for extension. The DNA sequences encoding the polypeptide monomers were optimized to match the codon preferences for *Escherichia coli*³⁸ as much as possible while incorporating restriction sites for DNA manipulation. Oligonucleotide synthesis and DNA sequencing were performed by Microsynth GmbH (Balgach, Switzerland). Western blots served to verify the presence of hexa- and pentahistidine epitopes in the recombinant target proteins (reducing SDS polyacrylamide gel electrophoresis (SDS-PAGE) with 18% acrylamide; primary antibody: QIA express anti-pentaHis antibody (Qiagen); secondary antibody: horseradish peroxidase-conjugated goat anti-mouse IgG; Sigma).

DNA Design. DNA Synthesis Encoding the Protein Monomers. The genes encoding the monomeric polypeptides (Chart 2A) were assembled by PCR procedures according to standard techniques and were adapted from Prodromou et al.³⁹ Briefly, single-stranded oligonucleotides (ca. 50 bp) representing the partial DNA sequence of each strand of the target polypeptide monomers (184 bp) were designed and chemically synthesized by Microsynth. These oligonucleotides have overlapping regions (15–18 bp) at their 3' ends with similar annealing temperatures. The whole double-stranded DNA segments encoding the protein monomers were extended from these oligonucleotides by PCR procedures. PCR products of target genes were purified by 2% low-melting agarose gels and subsequently extracted using a DNA extraction kit (Qiagen). After EcoR I and BamH I digestion (Boehringer Mannheim), the final constructs (184

Chart 2. (A) Gene^a Encoding the Assembled Monomers of the Target Protein Constructs and (B) Bst DSI-Digested Repeat Units Used for Multimerization



^a One letter base code: adenine (A), cytosine (C), guanine (G), and thymine (T).

bp) were cloned into a pUC 18 vector (Life Technologies, USA).

Multimerization of Polypeptide Monomers. After verification of the DNA sequence, the vector containing the full-size PCR product was amplified in 100 mL bacteria cultures (*E. coli*: TOPO 10 F', Invitrogen; LB medium containing 100 μ g/mL ampicillin) and purified using a Maxi-Kit (Qiagen). The repeat units (Chart 2B) were digested out of pUC 18 with BstDS I (Hybaid-AGS, Germany) and isolated from a 2% low melting point agarose gel and extracted using a DNA extraction kit (Qiagen). The purified monomeric DNA was self-ligated for 1.5–2 h at room temperature with T4 DNA ligase to form a population of multimers. The multimer mixtures were subsequently cloned into pUC 18 using the BstDS I sites and transformed into *E. coli* (TOPO 10 F'). Transformants were screened by restriction enzyme digest analysis (Eco RI and Bam HI), and the multimers of interest were subsequently cloned into the expression vector PET 14 b (Novagen) using the restriction sites Nde I and Bam HI (Boehringer Mannheim).

Protein Expression and Purification. Protein Expression. Expression vectors containing the DNA dimer and

tetramer (dimer and tetramer, respectively) were used to transform the bacterial expression host BL21(DE)pLys (Invitrogen). Pre-cultures were grown overnight at 37 °C in 100 mL of Luria–Bertani medium (LB) with selection by chloramphenicol (34 µg/mL) and ampicillin (100 µg/mL) and with rapid shaking. A total of 15 mL of the overnight culture was used to inoculate 1 L of LB medium for protein expression. Bacteria were grown to an OD at 600 nm of 0.850–0.950 in the presence of chloramphenicol and ampicillin, and protein expression was induced with 1 mM β -isopropyl thiogalactoside (IPTG). Expression of recombinant proteins was monitored by SDS–PAGE under reducing conditions followed by Coomassie staining. Cells were harvested after 4 h by centrifugation (6000 rpm, 20 min, 4 °C), and the pellets were stored at –80 °C.

Protein Purification. The multimeric target proteins have a thrombin-cleavable hexahistidine-tag (His-tag) at their N-termini provided by the PET 14b expression vector. The His-tag enables target protein purification from the bacterial lysate by Nickel-affinity chromatography. Briefly, each frozen cell pellet from 1 L of cell culture was thawed and resuspended in 80 mL of binding buffer (Novagen). The solution was incubated for 15 min at 37 °C with 250 mg/L lysozyme (Sigma). Benzoase (250 µL/L; Boeringer, Roche) was added to the lysate followed by being stirred at 6 °C for ca. 1.5–2 h. Insoluble proteins were separated from the lysate by centrifugation (14 000 rpm, 20 min, 4 °C). The target protein, which was soluble and mostly present in the supernatant, was purified by Nickel-affinity chromatography using nondenaturing conditions. Supernatant (ca. 320 mL) containing recombinant protein from 4 L of bacterial expression was purified with FPLC (Pharmacia) using a 2 × 5 L High Trap Chelating column (Pharmacia). After being loaded, the columns were washed several times with binding buffer at increasing imidazole concentrations (from 5 to 50 mM) to remove nonbinding proteins. The target protein was eluted from the column with 1 M imidazole and concentrated to a final protein concentration of 1–2 mg/mL. All purification steps were monitored by reducing SDS–PAGE. Finally, the target protein was dialyzed in dialysis bags (MW cutoff 6000–8000 Da; Spectrum Laboratories, Inc.) several times (7 × 5 L) against ddH₂O (pH 7.4) at 6 °C.

Protein Reduction. The reduction of intra- and intermolecular disulfide bonds was performed with tris(2-carboxyethyl)phosphine hydrochloride (TCEP·HCl, Pierce) using a molar excess of TCEP to cysteine residues of 1.5 and being incubated for 2 h at 25 °C (pH 6–7). The reducing agent was subsequently removed by dialysis in ddH₂O that had previously been degassed by being rinsed with argon for 1 h. The dialysis (6 × 3.5 L, over 9 h, 6 °C, pH 7) was performed by dialysis as described previously under oxygen-free conditions. The reduced protein was lyophilized and stored at –80 °C under argon.

Pooling of Protein Batches. Three to five batches of each protein expression were pooled. The lyophilized proteins were resuspended in degassed 6 mM triethanolamine (TEA) and 0.2 mM EDTA buffer (pH 6.8). TCEP was added to protein solutions of 1–2 mg/mL at a molar ratio of Cys/TCEP = 1:0.4. This solution was dialyzed against ddH₂O

(6 × 5 L, over 30 h, 6 °C, pH 6) as described previously. The proteins were lyophilized and stored at –80 °C under argon.

Protein Characterization. Total amino acid and mass spectrometry analysis were performed by the Protein Analysis Unit at the Institute of Biochemistry, University of Zurich (<http://www.biochem.unizh.ch/services/index.html>).

Detection of Free Thiols. Free thiols in reduced and nonreduced protein samples were measured using 7-diethylamino-3-(4'-maleimidylphenyl)-4-methylcoumarin (CPM, Molecular Probes). Fluorescence produced by CPM after reaction with free thiols can be monitored at the emission wavelength λ_{em} = 473 nm (excitation at λ_{ex} = 390 nm). The different protein polymers were compared with respect to their degree of reduction as measured by the amount of fluorescence. Concentration series ranging from 0.33 to 2 µM protein for the dimer construct and from 0.067 to 1.33 µM for the tetramer were reacted with an excess of CPM corresponding to theoretical thiols/CPM of at least a 1:15 molar ratio. The reactions (total volume of 150 µL, in nontransparent 96-well plates) were performed in HEPES buffered saline (50 mM HEPES, pH 8.1, 100 mM NaCl, 5 mM MgCl₂ 10% Glycerol⁴⁰) at room temperature (RT) for 4 h. Fluorescence was determined using an LS50B-Pekin-Elmer spectrofluorometer. The values shown in the charts are the mean of three to four samples at each concentration minus the background signal (blank) produced by nonreacted CPM in the reaction buffer. The same measurements were performed with reduced protein polymers that were first reacted with 2-hydroxy ethyl acrylate (HEA, Fluka) in a molar ratio of theoretical thiols/HEA of 1:10. This reaction was performed in HEPES buffered saline at RT for 2 h. The acrylate groups of HEA undergo a Michael-type addition with the protein thiols so they can no longer react with CPM. Ellman's reagent was also used to detect and determine free thiol content in the purified protein samples. The assay was performed as described in the product data sheet.⁴¹ Briefly, lyophilized protein polymers were resuspended in assay buffer and diluted to a range of concentrations. Ten to 15 min after the addition of Ellman's reagent to the protein solutions, the absorbance was measured at 412 nm with a UV-spectrophotometer (Perkin-Elmer, MBA 2000). The empirical absorption coefficient of 14150 M⁻¹ cm⁻¹ was used to determine the free thiol concentration in the different protein samples.

Biochemical Degradation of Protein Polymers. The recombinant protein polymers were characterized in terms of their degradability by human plasmin (Roche), human recombinant MMP-2 (matrix metalloproteinase 2 or gelatinase A, Oncogene), and MMP-1 (kindly provided by Dr. H. Nagase, Imperial College of Science, Technology, and Medicine, London). Lyophilized protein polymers were resuspended in enzyme buffers at concentrations of 1.6 mg/mL for plasmin degradation and 1.2 mg/mL for the two MMP degradation reactions, which corresponds to about 0.3 and 0.2 mM protein polymer, respectively (plasmin buffer: 20 mM Tris, 150 mM NaCl, pH 7.6; MMP buffers: 50 mM Tricine, 50 mM NaCl, 10 mM CaCl₂, and 0.05% Brij-35, pH 7.5). Plasmin (0.5 U/mL), MMP-1 (50 nM), and MMP-2

(2 nM) were incubated with the protein polymer solutions at 37 °C. Degradation products were visualized on Coomassie-stained 15% polyacrylamide reducing SDS-PAGE. For N-terminal sequencing (Protein Analysis Unit at the Institute of Biochemistry, University of Zurich), the degradation products were blotted to PVDF membrane (Bio-Rad Laboratories, Inc.). Ponceau stained bands were cut from the PVDF membrane and sent for N-terminal sequencing.

Functionalization of Poly(ethylene glycol) with Terminal Vinyl Sulfone Groups.

Materials. Poly(ethylene glycol) 6000 (PEG6000; M_n = 6000; Fluka, Switzerland), sodium hydride (powder, Aldrich), divinyl sulfone (Fluka, Switzerland), dichloromethane (Applichem, Germany), and diethyl ether (Fluka, Switzerland) were used without purification. Synthesis was adapted from Lutolf et al.⁹

Synthesis. A total of 5 g (0.84 mmol) of PEG6000 was dried by azeotropic distillation in 200 mL of toluene until complete evaporation of the solvent. After being cooled to room temperature, the PEG was dissolved in 400 mL of dichloromethane previously dried overnight on molecular sieves. A total of 0.2 g of sodium hydride was added (PEG/NaH of 1:10 molar ratio) to the PEG solution. After 30 min, 9 mL of divinyl sulfone was added (PEG/VS = 1:100 molar ratio). The reaction was allowed to proceed for 6 days at room temperature with stirring and was stopped by the addition of glacial acetic acid (acetic acid/NaH of 1:1 molar ratio). The resulting suspension was filtered through filter paper, and the solvent was partially evaporated to 30–40 mL. The product was precipitated by dropwise addition of the reaction solution to 500 mL of ice-cold diethyl ether. After recovery by filtration, the precipitate was washed with two volumes of diethyl ether and redissolved in 200 mL of dichloromethane. This solution was extracted with 200 mL of NaCl-saturated water, treated with activated carbon, filtered through filter-Celite (Macherey-Nagel, Germany), and finally dried over sodium sulfate. After the solvent was concentrated by rotary evaporation, the reaction product was precipitated in diethyl ether as described previously. The precipitate was extensively washed with diethyl ether and dried in vacuo. ¹H-NMR (CDCl₃) confirmed the desired reaction product, PEG6000-di-VS: δ = 3.7 ppm (PEG backbone), 6.1 ppm (CH₂=CH-SO₂, d, 2H), 6.4 ppm (CH₂=CH-SO₂, d, 2H), 6.8–6.9 ppm (CH₂=CH-SO₂, dd, 2H). The extent of end group conversion, as shown by NMR, was found to be 95 ± 2%, while the yield was about 75%.

Hydrogel Formation. Hydrogels were prepared by Michael-type addition of thiols (–SH) present in the protein polymers to vinyl sulfones (VS) at both termini of PEG6000-di-VS (Chart 1B,C). The precursors were resuspended in 0.45 M triethanolamine (TEA buffer, Aldrich) at desired concentrations and pH. For example, to make stoichiometrically balanced ($r = 1$ where $r = [\text{SH}]/[\text{VS}]$) 9.5% w/v gels, 2.01 mg of lyophilized protein dimer was dissolved in 30 μL of TEA buffer and mixed with 20 μL of a 0.128 mg/ μL PEG(6000)-di-VS solution. For the production of hydrogels at different stoichiometric ratios or containing the other protein polymers, the PEG6000-di-VS solution was kept

constant at 0.128 mg/ μL , while the protein solution was matched to the desired stoichiometry to form approximately 9.5% w/v hydrogels. Immediately after the mixing of the precursors, the solution was quickly vortexed, and drops of the reaction solution (25 μL) were transferred onto a sterile hydrophobic glass microscopy slide, obtained by treatment with SigmaCote (Sigma). Spacers of ca. 1 mm thickness were placed at both ends of the slide, and a second treated glass microscopy slide was positioned and clamped with binder clips over the lower one. The drop of precursor solution contacting only hydrophobic surfaces spread to form a disk. Hydrogels prepared at different precursor concentrations (i.e. 9.5, 7.5, and 5.5% w/v) were formed by concentrated precursor stock solutions being diluted to minimize weighing error. Mass % of precursors and r are specified for each individual hydrogel group. Although gelation occurred within a few minutes at 37 °C in a humidified incubator, the cross-linking reaction was allowed to proceed for about 1–2 h to achieve complete cross-linking.

Kinetics of Hydrogel Formation. The evolution of viscoelastic properties as reflected by the storage, G' , and loss modulus, G'' , as well as the phase angle, δ , defined as $\tan \delta = G''/G'$ during isothermal cross-linking at 23 °C were all recorded using a high-resolution rheometer (Bohling CVO 120) with parallel plate geometry (20 mm diameter). A total of 30 μL of premixed precursor solution was quickly pipetted between the two plates of the rheometer. After the upper plate was lowered to the experimental gap size (0.1 mm), rheological measurements were performed by a small strain oscillatory shear (strain = 0.05 and frequency = 0.5 Hz) being applied in a humidified atmosphere. The gel point (t_G), as a kinetic parameter for network formation, was recorded as the time point at which G' and G'' were congruent or at $\delta = 45^\circ$.

Equilibrium Swelling in PBS. Hydrogel disks (25 μL each), cast from one precursor solution, were swollen for at least 48 h in 3 mL of PBS (10 mM, pH 7.4; Sigma). After density determination⁹ by using an apposite kit on the basis of Archimedes' buoyancy principal (Toledo, Switzerland) and rheological investigation (see next section), gels were subsequently placed in 4 mL of deionized water to exclude salt from the dry mass for at least 48 h prior to lyophilization. The swelling ratio, Q_m , is defined herein as m_s/m_d , which is the mass ratio of networks at swelling equilibrium (m_s) and in the dry state (m_d), after freeze-drying. Q_m was used here as a comparative and representative simplification for swelling, instead of the volumetrically expressed ratio q , defined as the ratio of the gel volumes after swelling and of the dry network.⁴² The relationship between mass (Q_m) and volumetric swelling (q) is given by the ratio of the densities of gels in the swollen (δ_s) and dry (δ_d) state (i.e., $q = (\delta_d/\delta_s)Q_m$). According to the measured densities of swollen hydrogel groups (1.00 ± 0.005 and 1.01 ± 0.005 g/cm³ for degradable and for the nondegradable hydrogel groups, respectively; $n = 9$ –18; \pm standard deviation) and assuming that protein polymer densities are approximately the same, the ratio (δ_d/δ_s) should be constant for all the gel groups investigated; therefore, Q_m can be used as a representative swelling value.

Rheological Investigation of Swollen Hydrogels. Mechanical spectra of swollen hydrogels were obtained under small strain oscillatory shear at room temperature (23 °C). G' and G'' of swollen gels were measured at a constant strain of 0.05 and as a function of frequency (from 0.1 to 10 Hz). Hydrogels of 1–1.4 mm thickness were sandwiched between the two plates of the rheometer with compression up to 70% of their original thickness to avoid slipping.

For determining shear moduli of gels at equilibrium swelling in PBS (G'_e ; GG''_{ee}), preliminary investigations were performed to define the required measurement conditions. To achieve full contact between the hydrogel samples and the rheometer plates, the plate gap spacing was systematically decreased, and the hydrogel correspondingly compressed. Mechanical spectra were recorded at each gap size (plate distance). In agreement with Meyvis et al.,⁴³ the storage modulus reached a plateau, while the normal force increased as the gap size decreased (data not shown). This occurred at a penetration depth ranging from 15 to 30% of the original gel thickness depending on the hydrogel strengths. Mechanical properties at smaller gap sizes were not measured because plastic deformation or rupturing of gels would compromise the measurement.

Results and Discussion

Protein Polymers Designed for Hydrogel Formation.

The recombinant protein polymers described here were designed with the intention to react with PEG-di-VS upon two liquid precursor solutions being mixed, resulting in the formation of covalently cross-linked elastic hydrogels. Prerequisites for the achievement of this goal, applying the strategy illustrated in Chart 1B,C, include the solubility of the precursor materials (proteins and PEG) in aqueous buffers at convenient concentrations as well as the presence and accessibility of the reacting groups (thiols and vinyl sulfones) to enable the cross-linking reaction.

The solubility aspect of these protein polymers represents a potentially limiting factor in the design of recombinant proteins. Because of secondary and tertiary structure effects, it is difficult to predict whether a protein will be soluble under physiological conditions. However, there are known factors including overall charge and charge distribution in the protein backbone that may play an important role and that can be controlled rationally. Furthermore, the pH at which proteins are processed and cross-linked can strongly influence their solubility. On the other hand, protein folding and aggregation, which are also related to the amino acid composition and spatial distribution, simultaneously influence both the protein solubility and the accessibility of any functional groups (i.e., reactivity). The previous constraints are interconnected, and the complexity of balancing protein solubility and reactivity cannot be optimized independently. Our strategy for the design of such proteins was based on empirical observations. For solubility improvement, a sufficient number of amino acid residues had to be charged under physiological reaction conditions of pH 6–9, and those charged groups had to be sufficiently distributed along the protein backbone. Our choice of a charged amino acid for

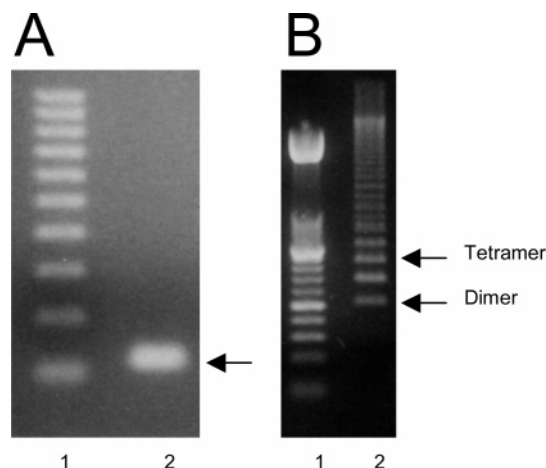


Figure 1. (A) Agarose gel (1.5%) showing Bst DSI-digested monomer DNA fragment encoding the repeat unit of the nondegradable or degradable construct (lane 2, arrow \leftarrow) running at about 126 bp according to the 100 bp DNA molecular weight ladder (lane 1). (B) Agarose gel (1.5%) illustrating a typical multimerization profile of the Bst DSI-digested DNA monomer sequence. DNA bands running as multiples of the BstDS I-digested monomer fragment (lane 2) in agreement with the 50 bp DNA molecular weight ladder (lane 1). Arrows (\leftarrow) show DNA bands of multimers used for investigation in the present work.

solubility purposes was the negatively charged glutamic acid (E). Glutamic acid was incorporated close to each of the cysteine residues, which are engaged in cross-linking (Chart 1A), thereby probably suppressing intermolecular protein aggregation and disulfide bond formation among thiols, both through electrostatic repulsion. In addition, glycine residues were incorporated as spacers between cysteines and neighboring glutamic acids to separate the negative charges from the thiol groups. This was based on the fact that a negatively charged environment in proximity of thiol groups will significantly slow the cross-linking reaction with divinyl sulfone groups or acrylates.³⁷

In conclusion, the presented protein polymers fulfill these *a priori* requirements, including overall solubility and the presentation of cross-linking groups to enable the formation of a covalently cross-linked hybrid polymer gel upon of the two components being mixed under appropriate conditions. The results shown next demonstrate that substitution of a few amino acids in the protein backbone can strongly influence the final material characteristics, including the elastic modulus and swelling, presumably because of changes in protein conformation.

Polymerization of DNA Monomers. As confirmed by DNA sequencing, the DNA sequences encoding the monomers of both degradable and nondegradable protein constructs were successfully produced from overlapping single-stranded DNA segments using either four polymerase chain reactions (PCRs) (for the degradable construct) or a single PCR (for the nondegradable one). Of note, the latter was shown to be a simple and straightforward method for the production of double-stranded artificial DNA.³⁹ BstDS I-digested monomer fragments (126 bp) can be seen as a single band in lane 2 of the agarose gel shown in Figure 1A. The nature of the nonpalindromic ends of the digested DNA monomers produced by BstDS I enables their multimerization as concatamers in a head-to-tail fashion (i.e.,

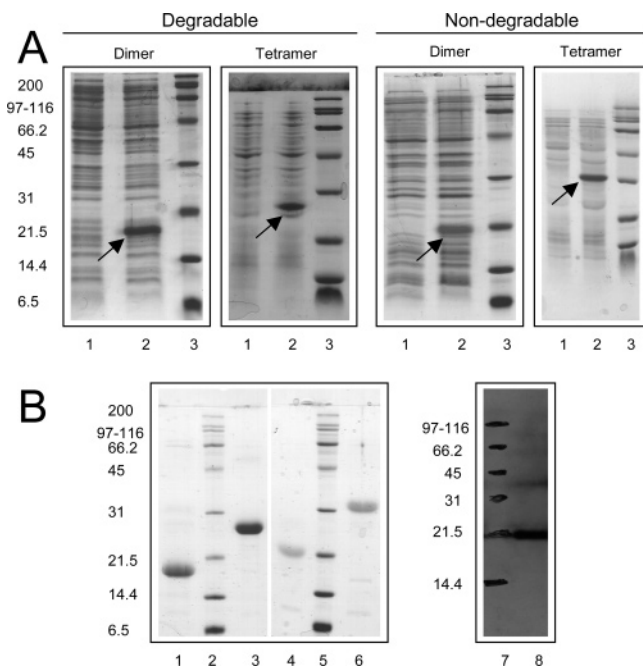


Figure 2. Coomassie-stained 15% reducing polyacrylamide SDS-PAGE documenting the bacterial expressed protein polymers. (A) Bacterial overexpression of the protein polymers (arrows). Lanes 1: complete bacterial lysate before induction with IPTG; lanes 2: complete bacterial lysate after 3 h induction with IPTG; and lanes 3: protein weight molecular marker broad range in kDa (prestained for dimers and normal for tetramers; Bio-rad). (B) Ni²⁺-affinity purified recombinant protein polymers. Lane 1: degradable dimer; lane 3: degradable tetramer; lane 4: nondegradable dimer; lane 6: nondegradable tetramer; lane 8: Western blot of the dimeric nondegradable protein from a 18% polyacrylamide SDS-PAGE, reacted with anti-penta-His antibody and visualized by chemiluminescence; and lanes 2, 5, and 7: molecular weight marker broad range in kDa (prestained; Bio-rad).

consistently in the correct 5' to 3' coding orientation only).^{20,21,24} Polymerization products of BstDS I-digested monomer fragments can be seen in lane 2 of the agarose gel shown in Figure 1B. These sizes of DNA bands clearly reflect multiples of the BstDS I-digested monomer fragment shown in lane 2 of Figure 1B. The DNA multimers used to express protein constructs in the present work (a DNA dimer of 252 bp and a DNA tetramer of 504 bp) are highlighted by arrows.

Protein Expression and Purification. As illustrated by the SDS-PAGE gel shown in Figure 2, all four protein polymers were successfully expressed using the PET expression system (Figure 2A) and readily purified (Figure 2B) using Ni²⁺-affinity chromatography. The yield was approximately 20–30 mg of purified protein from each liter of shaking-flask bacterial culture. According to the protein molecular weight markers used, the expression products migrate in reducing SDS-PAGE with a seemingly higher molecular weight than expected probably due to unresolved charge and solvent effects.²² The expected size and composition of the products was positively confirmed by mass spectroscopy (data not shown) and amino acid analysis. Under nondenaturing conditions, most of the recombinant target protein (>90%) was present in the soluble fraction of the bacterial lysate. Good solubility was also observed for the other three protein constructs (data not shown). The high solubility of these proteins in aqueous solutions was neces-

sary for their purification and further processing in the absence of denaturing agents such as urea. Bacterial expression and metal-affinity purification as performed in this study have served as a convenient and straightforward technique for the production of recombinant proteins.

Protein Characterization. Both total amino acid analysis (Table 1) and mass spectroscopy (data not shown) confirmed the identity of the target protein polymers. MALDI and ESI mass spectroscopy revealed two dominant peaks. The first peak was centered at a molecular mass corresponding to the theoretical protein mass reduced by the mass of a methionine residue. This is in accordance with the fact that in *E. coli*, N-terminal methionine residues incorporated during the translation initiation step are excised in close to 100% of the resulting proteins when the penultimate amino acid is small.^{44,45} In all protein constructs presented here, the penultimate residue is indeed the small amino acid glycine. The second main mass peak was found at about 178 Da larger than the first one and may correspond to a post-translational modification of the N-terminal polyhistidine tag, such as α -N-6-phosphogluconoylation, which occurs intrabacterially.⁴⁶ The presence of the polyhistidine tag in all of the target proteins was additionally confirmed by Western blotting using an anti-penta-His antibody (Figure 2B, lane 8).

The high water solubility at pH > 6 of all purified proteins was also preserved after dialysis against deionized H₂O prior to the reduction step, when the protein concentration is 1–2 mg/mL. Water solubility is an indispensable characteristic of these protein polymers for homogeneous, precipitation-free hydrogel formation. Furthermore, the observed water solubility validates our approach to improving protein solubility by adding charged amino acids, such as glutamic acid (E), to the protein backbone to increase the protein charge. Previous protein polymers from our group were not sufficiently soluble in aqueous solution in the absence of urea or without covalent modifications to ensure their solubility.⁷

Protein Polymers Display Free Thiols for Cross-Linking. The use of Ellman's assay (Figure 3A) revealed the presence of a small fraction of free thiols in protein polymers after Ni²⁺-affinity purification and dialysis of nonreduced protein polymers in deionized water, underlining the need for a reduction step in the preparation of protein polymers for cross-linking. The oxidation state of processed protein polymers (before and after the reduction step) was also investigated with CPM because of the high reaction selectivity of its maleimide group with thiol residues and its fluorescent properties.⁴⁷ Figure 3B,C shows the fluorescence intensity of CPM at the emission wavelength 473 nm (excitation wavelength 390 nm) after the reaction with thiol residues present in the recombinant protein at various concentrations. As previously reported⁴⁸ and in accordance with Figure 3B,C, the intensity of fluorescence increases linearly with protein concentration. Proteins that did not undergo the reduction step or reduced proteins previously reacted with HEA showed a significant drop of fluorescence intensity after the addition of CPM as compared to reduced proteins (Figure 3B). Thiols forming disulfide bonds

Table 1. Amino Acid Analysis of Produced Recombinant Proteins

amino acid ^a	degr. dimer			degr. tetramer			nondeg. diemr			nondegr. tetramer	
	theor. ^b	meas. ^c	SD	theor.	meas. ^c	SD	theor.	meas. ^c	SD	theor.	meas.
D + N ^d	12	13.9	1.0	24	26.8	0.6	14	15.3	1.4	28	30.1
E + Q ^d	16	16.4	1.2	28	30.0	0.5	14	13.9	1.6	24	25.5
S	11	13.8	1.7	17	14.1	3.9	13	13.4	1.3	21	19.9
H	10	8.3	0.6	12	11.2	0.3	10	8.0	0.9	12	10.8
G	30	31.6	1.4	52	52.8	0.4	32	31.3	0.5	56	55.8
T	2	2.4	0.5	4	4.2	0.7	2	2.1	0.7	4	4.7
A	4	5.2	0.2	8	8.9	0.7	4	4.7	0.4	8	9.1
R	7	6.7	0.3	13	13.1	0.7	3	3.0	0.4	5	6.2
Y	2	2.1	0.3	4	4.3	0.5	2	2.1	0.2	4	5.1
V	3	2.9	0.2	5	5.1	0.4	1	1.5	0.1	1	2.3
M	2	0.0	0.0	2	0.7	1.0	2	1.3	0.0	2	0.0
F	2	2.0	0.3	4	4.5	0.5	4	3.6	0.7	8	8.4
I	4	3.3	0.4	8	7.6	0.2	4	3.5	0.7	8	8.6
L	3	3.8	0.5	5	6.0	0.6	3	3.5	0.3	5	6.6
K	0	0.0	0.0	0	0.0	0.0	0	0.0		0	0.0
P	3	2.7	0.6	5	5.8	0.9	3	3.2	0.6	5	6.0
C ^e											

^a Alanine (A), arginine (R), asparagine and/or aspartic acid (N and/or D), cysteine (C), glutamic acid and/or glutamine (E and/or Q), glycine (G), histidine (H), isoleucine (I), leucine (L), lysine (R), methionine (M), phenylalanine (F), proline (P), serine (S), threonine (T), tryptophan (W), tyrosine (Y), valine (V). ^b Theor.: theoretical number of amino acids per macromolecule. ^c Average number of measured amino acids per molecule ($n = 3-4$) of the pooled protein polymers. SD = standard deviation. ^d As a result of hydrolysis prior to amino acid detection, asparagine and glutamine residues were converted into aspartic acid and glutamic acid, respectively. Therefore, the number of those residues detected reflects the number of original asparagine and aspartic acid residues (D + N), or glutamine and glutamic acid residues (E + Q), in the protein combined. ^e Cysteine residues are not quantifiable by the analysis.

(-S-S-, in nonreduced proteins) or thiols reacted with HEA can no longer react with CPM. These findings clearly confirm the stable presence of free thiol residues in the reduced target protein polymers. Moreover, reduced protein polymers containing the same number of repeat units (two or four, respectively) and differing only in their sensitivity to proteases display similar degrees of reduction (Figure 3C). These results are in agreement with those obtained from Ellman's assays (Figure 3A) and reconfirm the necessity of the reduction steps in the preparation of protein polymers for subsequence cross-linking to form hydrogel networks.

Recombinant Protein Polymers as Protease Substrates and Hydrogel Building Blocks. As expected, the protein constructs containing designed proteolytic cleavage sites were fully degradable. Figure 4 shows Coomassie-stained reducing SDS-PAGE gels of protein constructs and their degradation products after incubation with human MMP-1, MMP-2, and plasmin. Degradation by MMP-1 and MMP-2 was almost absent in control proteins containing inactive cleavage sites (nondegradable constructs, Figure 4B,D). The little degradation still observed on these proteins upon incubation with MMP-1 (Figure 4B,C) or with higher concentration of MMP-2 (data not shown) is probably due to the presence of cleavage sites for both MMPs, being less specific than the designed ones. However, these control proteins (nondegradable proteins) were rather unexpectedly degraded by plasmin. N-terminal sequencing of degradation products revealed that the C-terminus of the arginine residues (R), present in the protein backbone (Chart 1A), might serve as a plasmin degradation site. Each unit of the degradable target proteins contained two additional plasmin degradation sites, whereas the nondegradable construct only contained one such site, namely, at the RGD cell adhesion site. According to Hantgan et al.,³⁴ the cell adhesive sequence RGD is not noted as a

plasmin degradation site, probably because at the present conditions even less specific sites could be cleaved. However, arginine and lysine residues (at their C-termini) typically mark plasmin cleavage sites in proteins, at least to some extent, regardless of neighboring amino acids.⁴⁹ This is in agreement with our findings. N-terminal analysis confirmed the presence of a single MMP-1 site per monomeric unit in the degradable constructs, which is in accordance with Netzel-Arnett et al.³⁵

Because of multiple degradation sites in the proteins and different degradation products with similar molecular weights, it is difficult to identify discrete bands and correlate them to specific protein fragments. As shown in Figure 4, this issue was more significant in proteolytic degradation of tetrameric protein polymers with plasmin.

These findings clearly show the possibility of creating artificial proteins containing specific features, in this case, specificity to proteolytic degradation. However, additional undesired sites can be unexpectedly incorporated, challenging, to some extent, the design of these protein polymers.

Hydrogel Formation. Protein-co-PEG networks formed readily upon precursor solutions being mixed by Michael-type addition of cysteine thiols to vinyl sulfones of functionalized PEG as depicted in Chart 1C. Oscillatory shear moduli G' and G'' as well as the phase angle δ evolved typically for covalently cross-linking polymers as previously observed.^{9,50,51} The gel point t_G was extrapolated from rheological curves according to the criteria established by Chambon and Winter^{50,51} and here defined as the crossover of G' and G'' corresponding to $\delta = 45^\circ$. Each of the protein-co-PEG matrixes investigated herein reached their t_G within approximately 10 min at pH 7.7 and 23 °C. After reaching the gel point, both moduli continued to increase and leveled

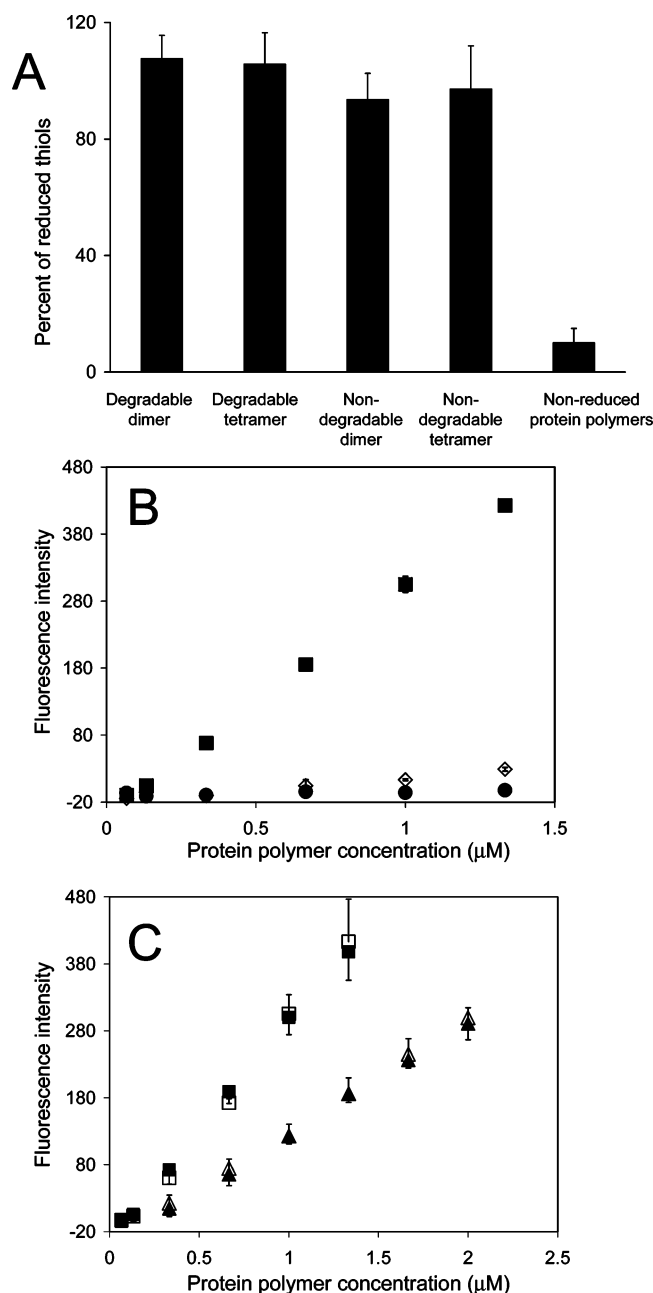


Figure 3. Detection of free thiols in processed protein polymers. (A) Ellman's assay. Measured free thiols in percentage of the number of cysteine residues (equal to the theoretical number of free thiols) present in the protein polymers ($n = 6$). Fluorescence intensity of CPM ($\lambda_{em} = 473$ nm and $\lambda_{ex} = 390$ nm) after reaction with free thiols present in the target protein polymers. (B) Reduced degradable tetramer (■), reduced degradable tetramer previously reacted with HEA (●), and nonreduced degradable tetramer (◇) [$n = 3$]. (C) Reduced degradable dimer (▲) [$n = 12$], reduced nondegradable dimer (△) [$n = 6$], reduced degradable tetramer (■) [$n = 12$], and reduced nondegradable tetramer (□) [$n = 6$]. Bars correspond to standard deviation. Average of n samples per point, and bars correspond to standard deviation.

off after ca. 1 h. Of note is that precursor solutions of up to 10% w/v protein only (i.e., lacking the co-reactive VS-functionalized PEG) did not gel via intermolecular disulfide bonding ($-S-S-$) at pH 7.7. However, this side reaction might occur during cross-linking, even in the presence of PEG-di-VS as shown for a similar system.⁹ Furthermore, the remarkable influence of the pH on the gelation rate and of the stoichiometry ratio ($r = SH/VS$) on the physicochemical

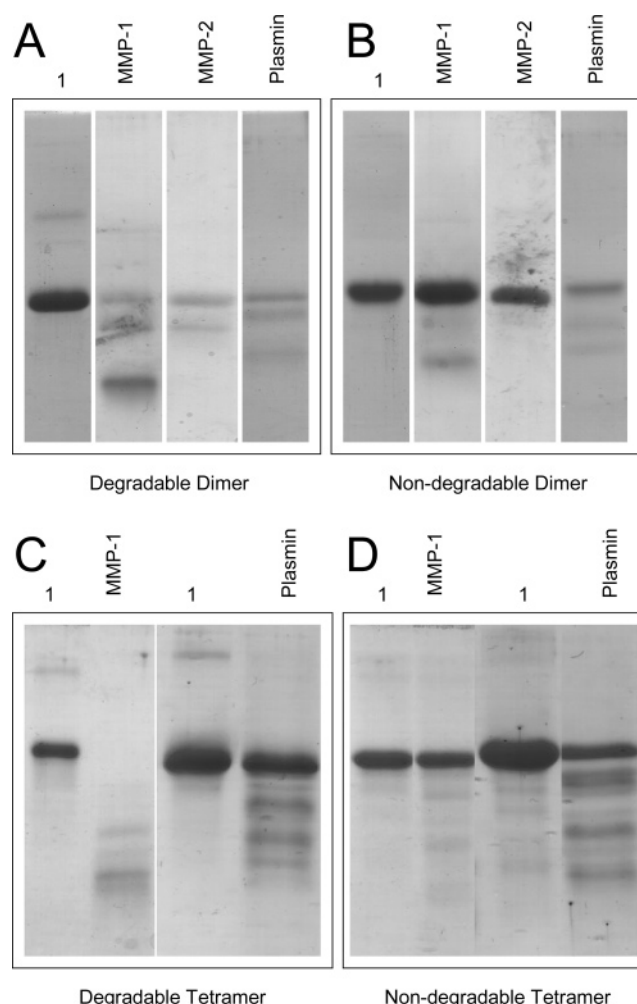


Figure 4. Coomassie-stained 15% reducing polyacrylamide SDS-PAGE illustrating proteolytic degradation of dimer (A and B) and of tetramer constructs (C and D) degradable and nondegradable, respectively. Protein polymers with both MMP-1 (50 nM) and MMP-2 (2 nM) were incubated at 37 °C for 7 days and with plasmin (0.5 U/mL) for 16 h. Lanes marked with 1 represent the corresponding protein polymer incubated for 7 days without the presence of proteases.

characteristics of the gels exclude other forms of hydrogel formation (e.g., physical).

Influence of pH on Gelation Rate. The rate of Michael-type addition of thiols to acrylates or vinyl sulfones is strongly dependent on pH and the particular pK_a of a given protein thiol^{9,37} since thiolates rather than thiols are the reacting species in this reaction. Lutolf et al.³⁷ altered the pK_a of thiols by modifying their local electrostatic environment via the addition of differently charged amino acids in the thiol's proximity. When positively charged amino acids were placed adjacent to the thiol-containing cysteine, a lower pK_a was obtained, and the thiol reacted faster at constant pH. Consequently, the charge of neighboring amino acids as well as changes in pH strongly affect the gelation time, t_g , of networks formed via Michael-type addition.⁹ Figure 5 shows the expected dependence of gelation rate on pH in our system. The time of gelation, t_g , also depends on the precursor's overall concentration (data not shown). Gelation occurred significantly faster at higher overall concentrations.

Factors that Influence Physicochemical Properties of Protein-co-PEG Hydrogels. The influence of stoichiometry

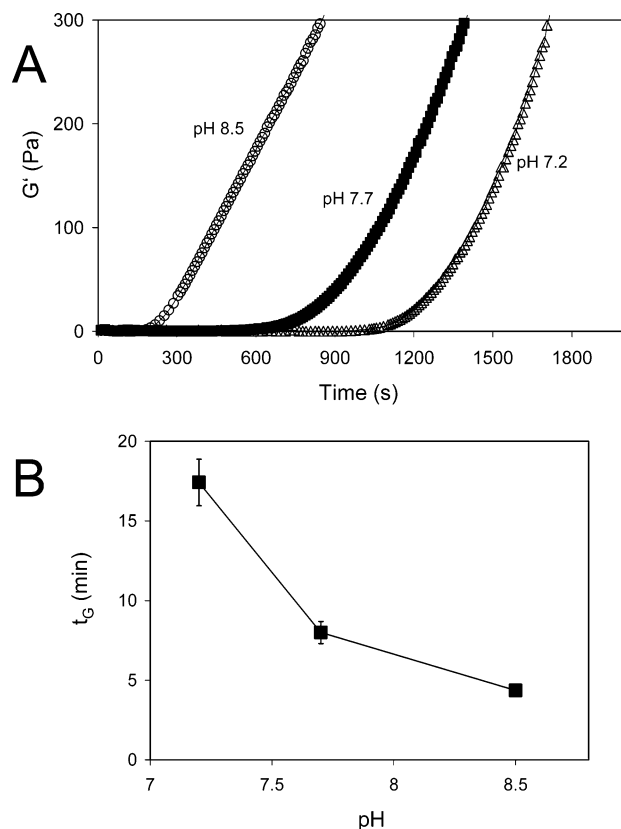


Figure 5. (A) pH dependence of storage modulus evolution (G') during in situ cross-linking. (B) Gel point (t_g = average of $n = 4 \pm$ standard deviation) as a function of pH (degradable dimer and PEG6000-di-VS system at 9.5% (w/v) precursor concentration).

of reacting groups and precursor concentration was analyzed in terms of equilibrium swelling and rheological properties after equilibrium swelling. These material characteristics and their dependence on preparation conditions are of fundamental importance in further investigations of hydrogels (e.g., with respect to cell–material interactions and three-dimensional cell migration that are currently under investigation). To ensure clinical relevance of these parameters, macroscopic material properties were determined in PBS at physiologic concentrations. Mechanical spectra of swollen hydrogels as illustrated in Figure 6 were used to extrapolate elastic modulus values. Shear moduli (G' and G'') as well as the phase angle (δ) were found to increase at higher frequencies. This behavior, due to network structure relaxation at higher frequencies, was normally observed to start approximately around 2–5 Hz. Values for G' shown here were generally taken from plateaus at frequencies between 0.1 and 1 Hz. In this range, hydrogels prepared at different precursor solution conditions showed predominantly viscous-elastic behavior (i.e., G' , G'' , and δ exhibited a plateau and were not frequency-dependent (Figure 6)).

Stoichiometry of Reacting Groups. The stoichiometry of reacting groups strongly influenced the macroscopic network properties, G'_e and Q_m (Figure 7). Hydrogels prepared with protein polymers and PEG6000-di-VS were evaluated at different molar ratios, r , of thiols to vinyl sulfones ranging from 0.8 to 1.53. Both degradable and nondegradable networks exhibited higher values for G'_e and lower values for Q_m when the precursor protein multimers

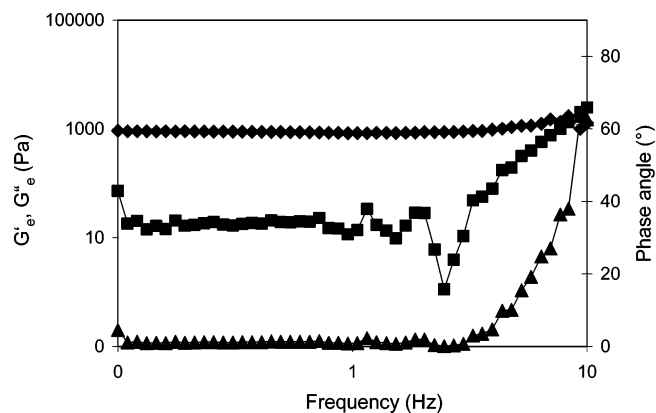


Figure 6. Typical mechanical spectra for swollen gels (nondegradable dimer and PEG6000-di-VS system) formed at 9.5% (w/v) precursor concentration and pH 7.7. G' (◆) showed a plateau over the investigated frequency range (0.1–10 Hz), and G'' (■) was generally around 2 orders of magnitude smaller than G' . However, G'' and the phase angle (▲) were seen to increase at higher frequencies (close to 10 Hz) depending on the preparation conditions of the hydrogels.

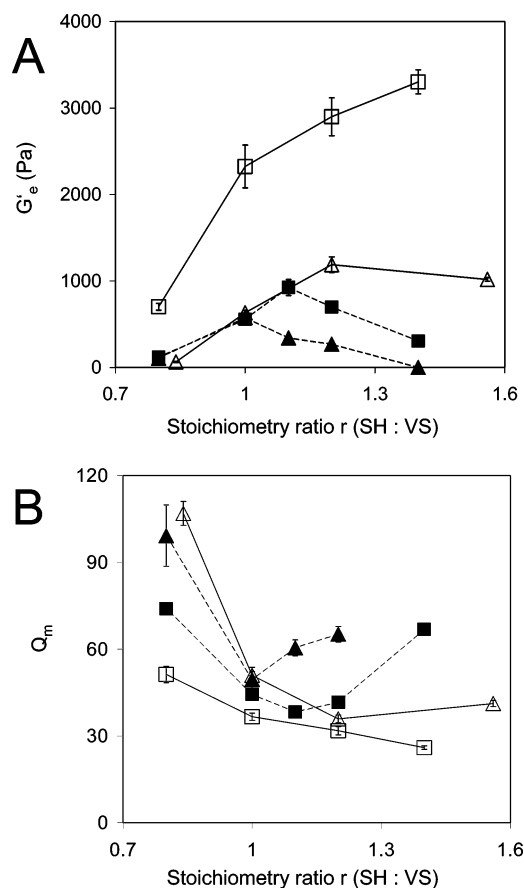


Figure 7. Influence of stoichiometric ratio r (SH/VS) on macroscopic network properties, specifically elastic moduli (A) and swelling (B), of hydrogels formed from PEG6000-di-VS and (▲) degradable dimer; (■) degradable tetramer; (△) degradable dimer; or (□) nondegradable tetramer. Normally, optimal macroscopic network properties (maximum values of G'_e and minimum values of Q_m , respectively) were obtained at $r > 1$ (r_{opt}). Average of $n \geq 4$ per point; bars correspond to standard deviation.

had high thiol content (i.e., with increasing protein monomeric units). The maximum of storage moduli values and the minimum of swelling degree, respectively, were generally observed at $r > 1$ ($r_{opt} > 1$), with the exception of hydrogels

formed with the degradable protein dimer, where $r_{\text{opt}} \cong 1$ (Figure 7). Furthermore, hydrogels formed from protein dimers reached r_{opt} at lower r as compared to hydrogels prepared with the tetramers of identical protein monomers.

It appeared that in general the need for an excess of cross-linkers to achieve optimal physicochemical properties is due to nonideal cross-linking behavior.^{52,53} Furthermore, poor accessibility of cross-linking sites during gelation, due to a decrease of diffusion of reactive groups and an increase in steric hindrance, respectively, could be an alternative explanation for the shift of r to values higher than 1.^{54,55} That could also be the reason that hydrogels prepared with tetramers had higher r_{opt} than networks formed from the dimers of the identical protein monomers. Additionally, the consumption of thiols by the formation of disulfide bonds⁹ might also account for suboptimal cross-linking efficiencies as reflected by low G'_e and high Q_m for $r = 1$ and therefore shifting the optimum (extremes) for G'_e and Q_m to higher values of r .

It is noteworthy that the dependence of G'_e and Q_m values on r differs among networks obtained from protein polymers with equal free thiol content (as confirmed by Ellman's and CPM assays, Figure 3). Furthermore, these differences are more pronounced with increasing numbers of monomer units in protein polymers (Figure 7). This inconsistency might be due to divergent behavior of nonidentical protein polymers at higher concentrations. Protein precursor solutions for hydrogel formation are more than one 100-fold more concentrated than for the CPM or Ellman's assay. For example, protein polymer gel precursor solutions containing degradable constructs were seen to precipitate overnight, whereas nondegradable protein constructs remained soluble for several days. Over longer time periods, intramolecular or intermolecular disulfide bond formation might alter the solubility of recombinant protein constructs in some cases. Furthermore, other unpredictable phenomena generated by the diversity of amino acids employed can occur in both protein constructs at high protein concentrations. They include a higher probability to conformational changes and aggregation of protein polymers. Protein conformation and aggregation could significantly limit access of thiols to vinyl sulfones and therefore could lead to inhomogeneous reactivity of thiols within a single protein backbone. A similar issue was previously raised by Halstenberg et al.⁷ Significant differences in gelation behavior of two analogous protein polymers differing only in a few amino acids were found. These differences were attributed to the different solubility of both protein polymers. Similarly, Urry et al. reported that the substitution of one or a few amino acids in only some repeat units of their protein polymers radically altered their properties.⁵⁶ These substitutions were made specifically with the purpose to develop materials with novel properties.

Precursor Concentration. The influence of precursor concentration (at r_{opt} and $r = 1.2$ for gels prepared formed with nondegradable tetramer protein) on the elastic modulus, G'_e , and swelling, Q_m , was investigated using gels prepared from precursor solutions with variable solid contents (5.5, 7.5, and 9.5% w/v). In general, elastic moduli increased, and swelling decreased with higher precursor concentrations

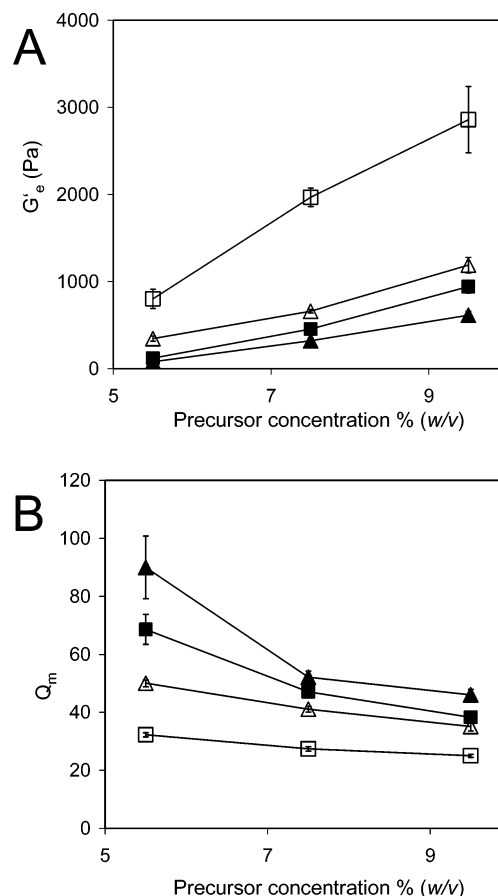


Figure 8. Dependence of macroscopic network properties, elastic moduli (A) and swelling (B), on the precursor concentration at r_{opt} (for tetramer nondegradable $r = 1.2$) for hydrogels formed from PEG6000-di-VS and degradable dimer (\blacktriangle); degradable tetramer (\blacksquare); degradable dimer (\triangle); or nondegradable tetramer (\square). Average of $n \geq 4$ per point; bars correspond to standard deviation.

(Figure 8) in accordance with the observations in similar systems.^{9,43} The differences in physicochemical properties of hydrogels prepared with protein multimers having equal numbers of cross-linking thiols persisted over the investigated range of precursor concentrations. However, the drop of shear moduli and the increase of swelling ratio, respectively, encountered for nondegradable systems at low precursor concentrations were more pronounced than for the degradable hydrogels. In particular, this effect was most evident in networks formed from nondegradable tetramer.

The dry mass ratio, defined as percent (w/w) of the lyophilized dry mass of networks after swelling over the mass of the solid components in the reaction mixture, was higher on average in the nondegradable matrixes, indicating that more precursor molecules participated in network formation (data not shown). At higher precursor concentrations, this could lead to entrapped entanglements acting as effective cross-links. On the other hand, either a smaller molecular weight, as in the case of the dimer nondegradable, or a lower dry mass ratio, as for both of the degradable protein constructs, could have reduced the effect of entanglements on the physicochemical gel properties.^{54,55,57,58}

Finally, the relationship between elastic modulus and swelling of previously characterized gels (Figure 8) was investigated. According to de Gennes,⁵⁹ the equilibrium swelling q and the elasticity of swollen hydrogels should

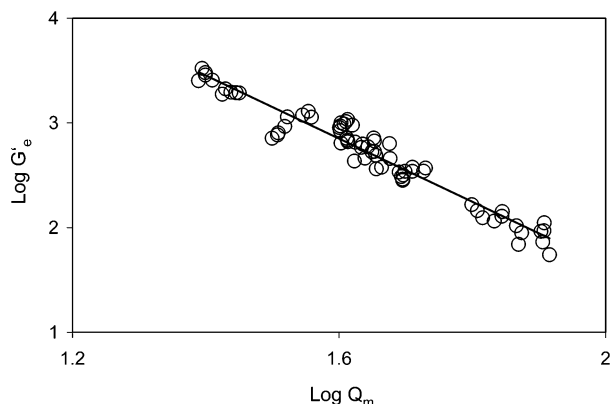


Figure 9. Double logarithmic plot of elastic moduli (G_e) at equilibrium swelling of individual gels prepared at different precursor concentrations as function of swelling (Q_m). A linear fit with a slope value of -3.04 (regression correlation coefficient: $r^2 = 0.942$) was calculated from the data confirming the theoretical power law connection between G_e and Q_m .

follow a power law. In agreement with this theory, a linear fit of the log–log plot of elastic moduli G_e as a function of equilibrium swelling Q_m for individual gels prepared with the different cross-linkers was observed (Figure 9). However, the exponent of the power law calculated here (around -3) deviates significantly from the theoretical value (-2.25). Similar empirical values were reported for other networks including randomly cross-linked dextran methacrylate swollen in aqueous buffers (-3.4),⁴³ end-linked poly(dimethylsiloxane) swollen in siloxane oligomer (-2.93),⁵⁷ and end-linked poly(ethylene glycol)-*co*-peptide swollen in water (-3).⁹ Deviations were partially attributable to the nonideal character of the networks including the presence of dangling ends.⁴³ Moreover, the nature of the solvent or the interaction between solvent and polymers can significantly influence the exponent of de Gennes's power law, allowing for the likely possibility that the value of -3 obtained here corresponds to polymer networks swollen in theta solvents.^{57,60} The consistency of our results with measurements of other network systems described in the literature validates the rheological characterization of our gels based on Meyvis et al.⁴³

Conclusion

We have presented the design of novel biomimetic PEG-protein matrixes formed by Michael-type conjugate addition. The mild nature of this cross-linking reaction and the possibility of controlling its rate via pH make it possible to transform liquid precursors into elastic solids under physiological conditions in situ. This scheme would potentially enable the intraoperative formation of synthetic biomaterials by mere injection into any kind of wound or tissue geometry. To address the clinical demand of injectable and bioactive materials for therapeutic tissue repair, recombinant protein polymers were rationally designed at amino acid level to meet, on one hand, prerequisites for hydrogel formation, including their solubility in aqueous buffers and the presence of cross-linking sites (i.e., thiols) and, on the other hand, to provide desired biological functionalities present in natural proteins, including cell adhesiveness and proteolytic sensitiv-

ity. In fact, genetic engineering allows, among other things, the bacterial production of artificial proteins with distinct characteristics and carrying combinations of functional domains derived from virtually any naturally occurring proteins. Controlling the physicochemical and biofunctional material properties strictly by protein polymer design remains a challenging but important task in light of future uses of biomimetic materials in a variety of tissue engineering and cell biological applications. Further systematic investigation of the biological functions of such materials, including the effects of different proteolytically sensitive domains and the behavior of incorporated growth factors, should provide important insights regarding the development of synthetic ECM analogues able to induce and respond to biological stimuli both in vitro and in vivo.

Acknowledgment. We thank Prof. Alyssa Panitch and Dr. Heike Hall for their scientific support and advice. We thank Dr. Peter Hunziker and Ragna Sack from the Protein Analysis Unit at the Institute of Biochemistry, University of Zurich for performing mass spectroscopy, total amino acid analysis, and N-terminal sequencing of proteins. We thank also Drs. Matthias P. Lutolf and Sven Halstenberg for manuscript revision and for constructive discussions and enhancements.

References and Notes

- Hubbell, J. A. *Biotechnology* **1995**, *13*, 565–576.
- Hubbell, J. A. *Curr. Opin. Solid State Mater. Sci.* **1998**, *3*, 246–251.
- Hubbell, J. A. *Curr. Opin. Biotechnol.* **1999**, *10*, 123–129.
- Griffith, L. G.; Naughton, G. *Science* **2002**, *295*, 1009.
- Langer, R.; Tirrell, D. A. *Nature* **2004**, *428*, 487–492.
- West, J. L.; Hubbell, J. A. *Macromolecules* **1999**, *32*, 241–244.
- Halstenberg, S.; Panitch, A.; Rizzi, S.; Hall, H.; Hubbell, J. A. *Biomacromolecules* **2002**, *3*, 710–723.
- Gobin, A. S.; West, J. L. *FASEB J.* **2002**, *16*, 751–753.
- Lutolf, M. P.; Hubbell, J. A. *Biomacromolecules* **2003**, *4*, 713–722.
- Lutolf, M. P.; Raeber, G. P.; Zisch, A. H.; Tirelli, N.; Hubbell, J. A. *Adv. Mater.* **2003**, *15*, 888.
- Chen, W. T. *Curr. Opin. Cell Biol.* **1992**, *4*, 802–809.
- Roskelley, C. D.; Srebrow, A.; Bissell, M. J. *Curr. Opin. Cell Biol.* **1995**, *7*, 736–747.
- Birkedal-Hansen, H. *Curr. Opin. Cell Biol.* **1995**, *7*, 728–735.
- Bannasch, H.; Horch, R. E.; Tanczos, E.; Stark, G. B. *Zentralbl. Chir.* **2000**, *125*, 79–81.
- Badiavas, E. V.; Paquette, D.; Carson, P.; Falanga, V. *J. Am. Acad. Dermatol.* **2002**, *46*, 524–530.
- Hutmacher, D. W.; Vanscheidt, W. *Drugs Today* **2002**, *38*, 113–133.
- Ellingsworth, L. R.; Delustro, F.; Brennan, J. E.; Sawamura, S.; McPherson, J. *J. Immunol.* **1986**, *136*, 877–882.
- Delustro, F.; Dasch, J.; Keefe, J.; Ellingsworth, L. *Clin. Orthop. Relat. Res.* **1990**, 263–279.
- Wang, C.; Stewart, R. J.; Kopecek, J. *Nature* **1999**, *397*, 417–420.
- McGrath, K. P.; Tirrell, D. A.; Kawai, M.; Mason, T. L.; Fournier, M. J. *Biotechnol. Prog.* **1990**, *6*, 188–192.
- McGrath, K. P.; Fournier, M. J.; Mason, T. L.; Tirrell, D. A. *J. Am. Chem. Soc.* **1992**, *114*, 727–733.
- Creel, H. S.; Fournier, M. J.; Mason, T. L.; Tirrell, D. A. *Macromolecules* **1991**, *24*, 1213–1214.
- McGrath, K. P.; Krejchi, M. T.; Borbely, J.; Fournier, M. J.; Mason, T. L.; Tirrell, D. A. *Mater. Res. Soc. Symp. Proc.* **1993**, *292*, 205–210.
- Cappello, J.; Crissman, J.; Dorman, M.; Mikolajczak, M.; Textor, G.; Marquet, M.; Ferrari, F. *Biotechnol. Prog.* **1990**, *6*, 198–202.
- Cappello, J. *Trends Biotechnol.* **1990**, *8*, 309–311.
- Ferrari, F.; Cappello, J. In *Protein-Based Materials*; Grath, K. M., Kaplan, D., Eds.; Birkhäuser: Boston, 1997; pp 37–60.
- O'Brien, J. P. *Trends Polym. Sci.* **1993**, *1*, 228–232.

- (28) Cappello, J. *MRS Bull.* **1992**, 17, 48–53.
- (29) Yu, S. M.; Conticello, V. P.; Zhang, G.; Kayser, C.; Fournier, M. J.; Mason, T. L.; Tirrell, D. A. *Nature* **1997**, 389, 167–170.
- (30) Petka, W. A.; Harden, J. L.; McGrath, K. P.; Wirtz, D.; Tirrell, D. A. *Science* **1998**, 281, 389–392.
- (31) Panitch, A.; Yamaoka, T.; Fournier, M. J.; Mason, T. L.; Tirrell, D. A. *Macromolecules* **1999**, 32, 1701–1703.
- (32) Welsh, E. R.; Tirrell, D. A. *Biomacromolecules* **2000**, 1, 23–30.
- (33) Friedl, P.; Bocker, E. B. *Cell. Mol. Life Sci.* **2000**, 57, 41–64.
- (34) Hantgan, R. R.; Francis, C. W.; Marder, V. J. In *Fibrinogen Structure and Physiology*, 3rd ed.; Colman, R. W., Hirsh, J., J., M. V.; Salzman, E. W., Eds.; J. B. Lippincott Company: Philadelphia, 1994; pp 277–300.
- (35) Netzel-Arnett, S.; Fields, G. B.; Birkedal-Hansen, H.; Van Wart, H. E.; Fields, G. *J. Biol. Chem.* **1991**, 266, 6747–6755.
- (36) Friedman, M.; Cavins, J. F.; Wall, J. S. *J. Am. Chem. Soc.* **1965**, 87, 3672.
- (37) Lutolf, M. P.; Tirelli, N.; Cerritelli, S.; Cavalli, L.; Hubbell, J. A. *Bioconjugate Chem.* **2001**, 12, 1051–1056.
- (38) Andersson, E.; Kurland, C. G. *Microbiol. Rev.* **1990**, 54, 198–210.
- (39) Prodromou, C.; Pearl, L. H. *Protein Eng.* **1992**, 5, 827–829.
- (40) Jezewska, M. J.; Rajendran, S.; Bujalowska, D.; Bujalowski, W. *J. Biol. Chem.* **1998**, 273, 10515–10529.
- (41) Ellman's Reagent, Instructions, Pierce Biotechnology; pp 1–4.
- (42) Flory, P. J. *Principles of Polymer Chemistry*; Cornell University Press: New York, 1953.
- (43) Meyvis, T. K. L.; De Smedt, S. C.; Demeester, J.; Hennink, W. E. *J. Rheol.* **1999**, 43, 933–950.
- (44) Hirel, P. H.; Schmitter, M. J.; Dessen, P.; Fayat, G.; Blanquet, S. *Proc. Natl. Acad. Sci. U.S.A.* **1989**, 86, 8247–8251.
- (45) Arnold, R. J.; Reilly, J. P. *Anal. Biochem.* **1999**, 269, 105–112.
- (46) Geoghegan, K. F.; Dixon, H. B.; Rosner, P. J.; Hoth, L. R.; Lanzetti, A. J.; Borzilleri, K. A.; Marr, E. S.; Pezzullo, L. H.; Martin, L. B.; LeMotte, P. K.; McColl, A. S.; Kamath, A. V.; Stroh, J. G. *Anal. Biochem.* **1999**, 267, 169–184.
- (47) Brinkley, M. *Bioconj. Chem.* **1992**, 3, 2–13.
- (48) Parvari, R.; Pecht, I.; Soreq, H. *Anal. Biochem.* **1983**, 22, 450–456.
- (49) Barrett, A. J.; Rawlings, N. D.; Woessner, J. F. *Handbook of Proteolytic Enzymes*; Academic Press: San Diego, 1998.
- (50) Chambon, F.; Winter, H. H. *Polym. Bull.* **1985**, 13, 499–503.
- (51) Winter, H. H.; Chambon, F. *J. Rheol.* **1986**, 30, 367–382.
- (52) Chambon, F.; Winter, H. H. *J. Rheol.* **1987**, 31, 683–697.
- (53) Winter, H. H.; Morganelli, P.; Chambon, F. *Macromolecules* **1988**, 21, 532–535.
- (54) Patel, S. K.; Malone, S.; Cohen, C.; Gillmor, J. R.; Colby, R. H. *Macromolecules* **1992**, 25, 5241–5251.
- (55) Urayama, K.; Kohjiya, S. *J. Chem. Phys.* **1996**, 104, 3352–3359.
- (56) Urry, D. W.; Peng, S. Q.; Hayes, L. C.; McPherson, D.; Xu, J.; Woods, T. C.; Gowda, D. C.; Pattanaik, A. *Biotechnol. Bioeng.* **1998**, 58, 175–190.
- (57) Sivasailam, K.; Cohen, C. *J. Rheol.* **2000**, 44, 897–915.
- (58) Urayama, K.; Kawamura, T.; Kohjiya, S. *J. Chem. Phys.* **1996**, 105, 4833–4840.
- (59) De Gennes, P. G. *Scaling Concepts in Polymer Physics*; Cornell University: Ithaca, NY, 1979.
- (60) Zrinyi, M.; Horkay, F. *Macromolecules* **1984**, 17, 2805–2811.

BM049614C